Algebraic Differential Kinematics of Planar 4R Linkages

M. John D. Hayes[1], Mirja Rotzoll[2], Atena E. Iraei[3], Alia Nichol[3], and Quinn Bucciol[3]

Abstract— **In this paper some new and some already established results are discussed which are ideally suited for teaching four-bar mechanism kinematics to senior undergraduate mechanical engineering students. We re-examine the velocity and acceleration level kinematics of planar 4R linkages for the six distinct angle pairings of the four link orientation angles, θ_i-θ_j, in the light of the first two time derivatives of the resulting algebraic equations. Freudenstein's Theorem 1, which states that the angular velocity ratio of the two ground-fixed moving links is equivalent to a ratio of the three instantaneous centres of velocity aligned on the line joining the centres of the two ground-fixed R-pairs, is re-expressed in terms of the coupler line equation via the algebraic input-output (IO) equation, and confirmed using the first time derivative of the same equation. We prove that similar ratios can be easily obtained for the five other distinct IO equations for any planar 4R linkage. A clear advantage of our novel approach is that we obtain six signed ratios, thereby indicating the relative sense of the angular velocities, whereas the generalised Freudenstein theorem 1 reveals only four. We next identify conditions for minimum and maximum angular velocities and propose a corollary to Freudenstein's Theorem 2. Finally, we investigate the acceleration level kinematics for all six IO equations, determine extreme values, and discuss implications for extreme values of torque and force transfer as well as shaking forces.**

I. INTRODUCTION

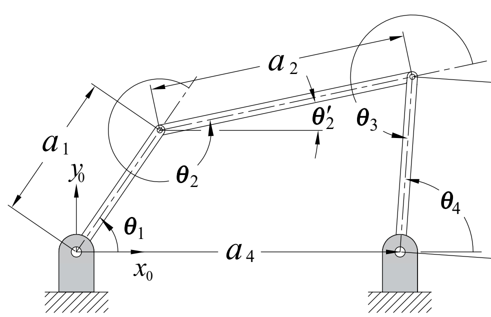

Fig. 1. Planar 4R simple closed kinematic chain.

The standard modern input-output (IO) equation for a planar 4R linkage is the well known Freudenstein equation [1]

$$k_1 + k_2 \cos\theta_4 - k_3 \cos\theta_1 \quad = \quad \cos(\theta_4 - \theta_1), \qquad (1)$$

where the four link length parameters are a_1, a_2, a_3, and a_4 while the IO angles are θ_1 and θ_4, respectively, see Figure 1 for reference. The Freudenstein parameters are defined as:

$$k_1 = \frac{a_1^2 - a_2^2 + a_3^2 + a_4^2}{2a_1a_3}, \quad k_2 = \frac{a_4}{a_1}, \quad k_3 = \frac{a_4}{a_3}. \qquad (2)$$

It is always possible, employing the laws of sines and cosines, to obtain any of the six possible angle pair IO equations, though it is rarely done. Employing trigonometry and using the Freudenstein approach means that absolute angles expressed in a single fixed coordinate system must be used. For example, we could obtain an IO equation between θ_1 and θ_2' where both angles are measured with respect to the positive x_0-axis in Figure 1. An example found in [2] gives

$$k_1 \cos\theta_2' + k_4 \cos\theta_1 + k_5 \quad = \quad \cos(\theta_1 - \theta_2'). \qquad (3)$$

It is important to note that $\theta_2 \neq \theta_2'$ because θ_2 is the angle the coupler, a_2, makes with respect to the input link, a_1. However, because all angles in Equation (3) are expressed with respect to the positive x_0-axis the two new Freudenstein parameters, k_4 and k_5, have different definitions from k_2 and k_3 in Equation (1), namely

$$k_4 = \frac{a_4}{a_2}, \quad k_5 = \frac{a_3^2 - a_1^2 - a_2^2 - a_4^2}{2a_1a_2}. \qquad (4)$$

This means that arbitrary angle pairings will lead to markedly different coefficients as parameters.

While there are other new approaches [3], [4], we believe those presented here are the simplest and most uniformly comprehensive. In this paper, we define the angles as tangent half-angle parameters v_i of the four θ_i joint angles as measured in Figure 1. The novel application of an algorithm developed in [5] and applied in a unique way in a companion paper [6] reveals the v_i-v_j IO equations for all six angle parameter pairings in a planar 4R linkage leading to six distinct algebraic IO equations where all coefficients are defined in precisely the same way, but permuted in distinct different ways in the six equations. Our objective is to re-examine the velocity and acceleration level kinematics with these equations, and to apply the results to mechanism design and analysis, but also to teaching mechanism kinematics to senior mechanical engineering undergraduate students.

II. POSITION LEVEL KINEMATICS

The six distinct IO equations relating the six distinct v_i-v_j angle parameter pairings found in [6] are slightly different from those presented here. Because of the derivation algorithm, the ground fixed relatively non-moving coordinate system attached to the centre of the R-pair connecting a_1 to a_4 is rotated by π radians compared to the x_0-y_0 coordinate

[1]Professor, Department of Mechanical and Aerospace Engineering, Carleton University, Ottawa, ON, Canada, john.hayes@carleton.ca
[2]Ph.D. Candidate, Department of Mechanical and Aerospace Engineering, Carleton University, Ottawa, ON, Canada, mirja.rotzoll@carleton.ca
[3]Undergraduate Student, Department of Mechanical and Aerospace Engineering, Carleton University, Ottawa, ON, Canada, atena.iraei, alia.nichol, quinn.bucciol@carleton.ca

system illustrated in Figure 1. For research purposes, the fixed coordinate reference system orientation is arbitrary. However, in order to use this material to teach a senior undergraduate one-semester course in mechanism and machine theory to mechanical engineering students, the reference coordinate system, and hence the equations, should be rotated to the typical form with x_0 pointing to the right and y_0 pointing up. The appropriately rotated v_1-v_4 IO equation is

$$Av_1^2v_4^2 + Bv_1^2 + Cv_4^2 - 8a_1a_3v_1v_4 + D = 0, \tag{5}$$

where

$$\begin{aligned}
A = A_1A_2 &= (a_1 - a_2 - a_3 + a_4)(a_1 + a_2 - a_3 + a_4),\\
B = B_1B_2 &= (a_1 - a_2 + a_3 + a_4)(a_1 + a_2 + a_3 + a_4),\\
C = C_1C_2 &= (a_1 - a_2 + a_3 - a_4)(a_1 + a_2 + a_3 - a_4),\\
D = D_1D_2 &= (a_1 + a_2 - a_3 - a_4)(a_1 - a_2 - a_3 - a_4),\\
v_1 &= \tan\tfrac{\theta_1}{2},\\
v_4 &= \tan\tfrac{\theta_4}{2}.
\end{aligned}$$

The remaining five are

$$A_1B_1v_1^2v_2^2 + A_2B_2v_1^2 + C_1D_2v_2^2 + 8a_2a_4v_1v_2 + C_2D_1 = 0, \tag{6}$$

$$A_2B_1v_1^2v_3^2 + A_1B_2v_1^2 + C_1D_1v_3^2 + C_2D_2 = 0, \tag{7}$$

$$B_1C_1v_2^2v_3^2 + A_1D_2v_2^2 + A_2D_1v_3^2 - 8a_1a_3v_2v_3 + B_2C_2 = 0, \tag{8}$$

$$A_1C_1v_2^2v_4^2 + B_1D_2v_2^2 + A_2C_2v_4^2 + B_2D_1 = 0, \tag{9}$$

$$A_2C_1v_3^2v_4^2 + B_1D_1v_3^2 + A_1C_2v_4^2 - 8a_2a_4v_3v_4 + B_2D_2 = 0. \tag{10}$$

III. Velocity Level Kinematics

The equation relating the time rates of change of the joint angle parameters v_1 and v_4 can be determined as the first time derivative of Equation (5):

$$\big((Av_4^2 + B)v_1 - 4a_1a_3v_4\big)\dot{v}_1 + \big((Av_1^2 + C)v_4 - 4a_1a_3v_1\big)\dot{v}_4. \tag{11}$$

Because Equation (11) equates to zero, the velocity parameter ratio can be expressed as

$$\frac{\dot{v}_4}{\dot{v}_1} = -\frac{(Av_4^2 + B)v_1 - 4a_1a_3v_4}{(Av_1^2 + C)v_4 - 4a_1a_3v_1}, \tag{12}$$

which can also be directly obtained as the implicit derivatives of Equation (5) with respect to v_1 and v_4. It is important to note that for the i^{th} link, $\dot{v}_i \neq \dot{\theta}_i$ since $v_i = \tan(\theta_i/2)$. But it is a simple matter to show that

$$\dot{v}_i = \frac{\dot{\theta}_i(1 + v_i^2)}{2}, \tag{13}$$

and that

$$\dot{\theta}_i = \frac{2\dot{v}_i}{(1 + v_i^2)}. \tag{14}$$

Hence, the reciprocal of the mechanical advantage is

$$\frac{\dot{\theta}_4}{\dot{\theta}_1} = -\frac{((Av_4^2 + B)v_1 - 4a_1a_3v_4)(1 + v_1^2)}{((Av_1^2 + C)v_4 - 4a_1a_3v_1)(1 + v_4^2)}. \tag{15}$$

The remaining velocity parameter equations are expressed as the following ratios

$$\frac{\dot{v}_2}{\dot{v}_1} = -\frac{(A_1B_1v_2^2 + A_2B_2)v_1 + 4a_2a_4v_2}{(A_1B_1v_1^2 + C_1D_2)v_2 + 4a_2a_4v_1}, \tag{16}$$

$$\frac{\dot{v}_3}{\dot{v}_1} = -\frac{(A_2B_1v_3^2 + A_1B_2)v_1}{(A_2B_1v_1^2 + C_1D_1)v_3}, \tag{17}$$

$$\frac{\dot{v}_3}{\dot{v}_2} = -\frac{(B_1C_1v_3^2 + A_1D_2)v_2 - 4a_2a_4v_3}{(B_1C_1v_2^2 + A_2D_1)v_3 - 4a_2a_4v_2}, \tag{18}$$

$$\frac{\dot{v}_4}{\dot{v}_2} = -\frac{(A_1C_1v_4^2 + B_1D_2)v_2}{(A_1C_1v_2^2 + A_2C_2)v_4}, \tag{19}$$

$$\frac{\dot{v}_4}{\dot{v}_3} = -\frac{(A_2C_1v_4^2 + B_1D_1)v_3 - 4a_2a_4v_4}{(A_2C_1v_3^2 + A_1C_2)v_4 - 4a_2a_4v_3}, \tag{20}$$

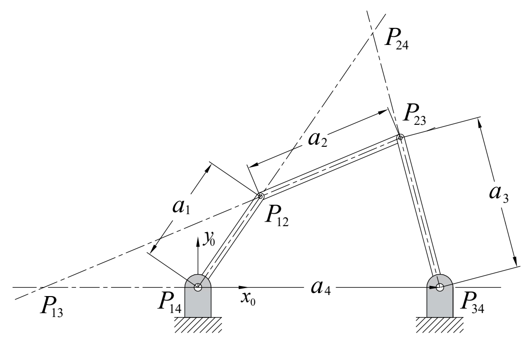

Fig. 2. The six instantaneous centres of velocity.

IV. Generalisation of Freudenstein's Theorem 1

Consider the planar 4R linkage illustrated in Figure 2. It is well known that as the 4R linkage moves it has four primary instantaneous centres of velocity (ICV), one at the centre of each R-pair. Two of the primary ICVs, P_{12} and P_{23}, move on centrodes defined by the link lengths, while P_{14} and P_{34} are stationary. The two secondary ICVs are P_{13} and P_{24}, which also move on centrodes. By virtue of the Aronhold-Kennedy theorem, P_{13}, P_{14}, and P_{34} remain collinear as the motion evolves over time meaning that the centrode for P_{13} is a segment of the line joining the two ground-fixed R-pairs, the x_0-axis, and is located at the point of intersection of the x_0-axis and the extension of the centreline of the coupler, a_2. Freudenstein's Theorem 1 [7], [8] states that the value of the ratio of the output angular velocity and the input angular velocity, $\dot{\theta}_4$ and $\dot{\theta}_1$, can be expressed by the ratio of the values of the relative directed distances between the three ICVs located on the x_0-axis in the following way:

$$\frac{\dot{\theta}_4}{\dot{\theta}_1} = \frac{d_{P_{13}P_{14}}}{d_{P_{13}P_{14}} + d_{P_{14}P_{34}}}, \tag{21}$$

where the directed distances $d_{P_{14}P_{34}}$ and $d_{P_{13}P_{14}}$ can be positive or negative depending on their relative directions.

It is a straightforward computation to express the value of the location of P_{13} as the point of intersection of the longitudinal centreline of the coupler and the line containing the x_0-axis in terms of the link directed lengths and the joint angle parameters v_1 and v_4 as

$$\frac{\left(\frac{a_1\left(a_3v_1^2v_4-a_3v_1v_4^2+a_4v_1v_4^2+a_3v_1-a_3v_4+a_4v_1\right)}{a_1v_1v_4^2-a_3v_1^2v_4+a_1v_1-a_3v_4}\right)}{\left(\frac{a_1\left(a_3v_1^2v_4-a_3v_1v_4^2+a_4v_1v_4^2+a_3v_1-a_3v_4+a_4v_1\right)}{a_1v_1v_4^2-a_3v_1^2v_4+a_1v_1-a_3v_4}+a_4\right)}. \quad (22)$$

Selecting a configuration of a viable planar 4R and substituting the appropriate values one may easily see that the values of Equations (15), (21), and (22) are equivalent. For example, substituting the a_i values of $a_1 = 7$, $a_2 = 13$, $a_3 = 8$, $a_4 = 16$, $v_1 = \tan(60°/2)$ and $v_4 = \tan(87.4498°/2)$ into the three equations leads to the identical result

$$\frac{\dot{v}_4(1+v_1^2)}{\dot{v}_1(1+v_4^2)} \quad = \quad 0.6974. \quad (23)$$

However, Freudenstein's first theorem also applies to the ICVs on each of the three other Aronhold-Kennedy lines of three collinear ICVs with respect to a number line coincident with the line of three ICVs having its origin on the central ICV. It seems that, to the best of the authors collective knowledge, this fact has never been discussed in the literature. The six ICVs are known as *velocity poles* and the curves they move along are described as *polodes*, see [9], [10], [11], [12] for example. However, it seems that the following three velocity ratios expressed as ratios of the absolute values of the relative locations of the three ICVs on the three other Aronhold-Kennedy lines, see Figure 2, have never been stated explicitly as:

$$\frac{\dot{\theta}_1}{\dot{\theta}_2} \quad = \quad \frac{d_{P_{24}P_{12}}}{d_{P_{24}P_{12}} + d_{P_{12}P_{14}}}; \quad (24)$$

$$\frac{\dot{\theta}_3}{\dot{\theta}_2} \quad = \quad \frac{d_{P_{13}P_{12}}}{d_{P_{13}P_{12}} + d_{P_{12}P_{23}}}; \quad (25)$$

$$\frac{\dot{\theta}_4}{\dot{\theta}_3} \quad = \quad \frac{d_{P_{24}P_{23}}}{d_{P_{24}P_{23}} + d_{P_{23}P_{34}}}. \quad (26)$$

Additionally, Equations (17) and (19) can be similarly expressed as angular velocity ratios in terms of distance and configuration as:

$$\frac{\dot{\theta}_3}{\dot{\theta}_1} \quad = \quad -\frac{((A_2B_1v_3^2 + A_1B_2)v_1)(1+v_1^2)}{((A_2B_1v_1^2 + C_1D_1)v_3)(1+v_3^2)}; \quad (27)$$

$$\frac{\dot{\theta}_4}{\dot{\theta}_2} \quad = \quad -\frac{((A_1C_1v_4^2 + B_1D_2)v_2)(1+v_2^2)}{((A_1C_1v_2^2 + A_2C_2)v_4)(1+v_4^2)}. \quad (28)$$

In addition to Equation (12), these results yield a measure of all six velocity parameter ratios with the five additional Equations (16)-(20).

A. Example: Velocity Ratio

In this section we shall illustrate the validity of our generalised Freudenstein theorem ratios of relative distances between ICVs on the four Aronhold-Kennedy lines and explicitly computed angular velocity ratios. For this example the linkage and configuration illustrated in Figure 2 are used with the lengths (generic units) and angles (degrees) listed in Table I.

Using these parameters, the four Aronhold-Kennedy lines, and the extended Freudenstein theorem yields:

$$\left.\begin{array}{ccccc}
\frac{d_{P_{13}P_{14}}}{d_{P_{13}P_{14}} + d_{P_{14}P_{34}}} & = & 1.0657 & = & \frac{\dot{\theta}_4}{\dot{\theta}_1}; \\
\frac{d_{P_{24}P_{12}}}{d_{P_{24}P_{12}} + d_{P_{14}P_{12}}} & = & -3.9492 & = & \frac{\dot{\theta}_1}{\dot{\theta}_2}; \\
\frac{d_{P_{13}P_{12}}}{d_{P_{13}P_{12}} + d_{P_{12}P_{23}}} & = & -1.2595 & = & \frac{\dot{\theta}_3}{\dot{\theta}_2}; \\
\frac{d_{P_{24}P_{23}}}{d_{P_{24}P_{23}} + d_{P_{23}P_{34}}} & = & 3.3419 & = & \frac{\dot{\theta}_4}{\dot{\theta}_3}.
\end{array}\right\} \quad (29)$$

The negative or positive sign multiplying the ratio indicates whether or not the two angular velocities have the same sense. Compared to the angular velocities obtained with the six angular velocity ratios computed with suitable variants of Equation (15), we obtain four identical ratios in addition to two, which are not possible to compute directly as ratios of ICVs:

$$\left.\begin{array}{ll}
\frac{\dot{\theta}_4}{\dot{\theta}_1} = 1.0657; & \frac{\dot{\theta}_3}{\dot{\theta}_2} = -1.2595; \\
\frac{\dot{\theta}_1}{\dot{\theta}_2} = -3.9492; & \frac{\dot{\theta}_4}{\dot{\theta}_2} = -4.2085; \\
\frac{\dot{\theta}_3}{\dot{\theta}_1} = 0.3189; & \frac{\dot{\theta}_4}{\dot{\theta}_3} = 3.3419.
\end{array}\right\} \quad (30)$$

TABLE I
CONFIGURATION PARAMETERS FOR A CLOSED 4R CHAIN.

Parameter	Dimension	Parameter	Dimension
a_1	5	$d_{P_{13}P_{14}}$	-32.4571
a_2	6	$d_{P_{13}P_{12}}$	-29.1205
a_3	8	$d_{P_{24}P_{12}}$	6.6954
a_4	2	$d_{P_{24}P_{23}}$	11.4161
θ_1	45°	θ_3	207.5141°
θ_2	308.0304°	θ_4	20.5445°

V. COROLLARY TO FREUDENSTEIN'S THEOREM 2

Freudenstein's second theorem [7], [8] states that *at an extreme value of the velocity ratio in a four-bar linkage, the collineation axis is perpendicular to the longitudinal centreline of the coupler*. The collineation axis is defined

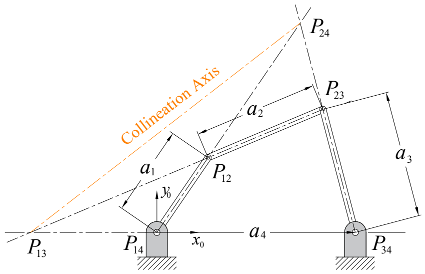

Fig. 3. The collineation axis.

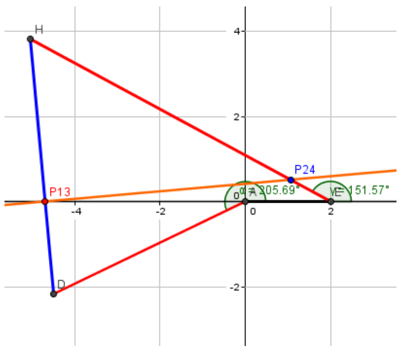

Fig. 4. The collineation axis is perpendicular to the coupler.

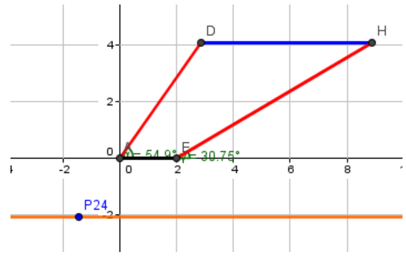

Fig. 5. The collineation axis and coupler are parallel to the x_0-axis, the linkage is a convex quadrangle.

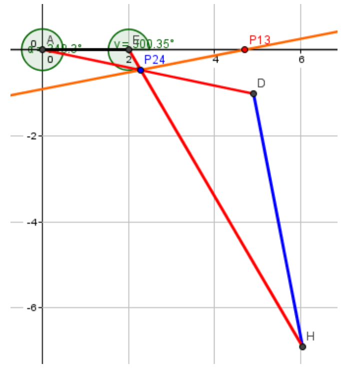

Fig. 6. The collineation axis is again perpendicular to the coupler.

to be the line containing the two secondary ICVs, P_{13} and P_{24}, see Figure 3.

We propose the following corollary to Freudenstein's Theorem 2: *the velocity ratio becomes unity in a four-bar linkage when the collineation axis and the coupler centre line are parallel to the x_0-axis*. Figures 4 and 5 illustrate instances of Theorem 2, and it's corollary being true. To prove the corollary it suffices to consider a drag-link (double crank) planar 4R with a_4 being the shortest link. In this Grasshof inversion case, the coupler can rotate freely through 2π radians and the coupler must therefore align with the x_0-axis direction in two configurations in each of two assembly modes. Figure 5 illustrates one such configuration placing P_{13} at infinity. If the link lengths can form a convex quadrangle in one of these configurations, in the other, of the same assembly mode, it forms a complex quadrangle where a_1 and a_3 cross each other. A configuration illustrating a complex quadrangle appears in Figure 7.

To identify the locations of the positions of P_{13} where it is instantaneously at rest and changing directions on the x_0-axis, we require the longitudinal centreline equation of the coupler to determine its point of intersection with the x_0-axis. Using the point-slope form of the planar line equation it is a simple matter to compute the location of P_{13} given any value v_1 and the corresponding value of v_4 revealing

$$P_{13} = \frac{a_1(a_3v_1^2v_4+(a_4-a_3)v_1v_4^2+(a_3+a_4)v_1-a_3v_4)}{a_1v_1v_4^2-a_3v_1^2v_4+a_1v_1-a_3v_1}. \quad (31)$$

We now solve Equation (5) for v_4 and substitute the results back into Equation (31) yielding two equations for P_{13} in terms of v_1, one corresponding to each assembly mode. Next, we identify the critical values of v_1 revealing the extreme locations of P_{13}. These critical values are obtained by setting the derivative of the equation with respect to v_1 equal to 0 and computing $v_{1_{\text{crit}}}$ as:

$$\frac{dP_{13}}{dv_1} = 0. \quad (32)$$

Equation (32) is of degree 6 in v_1 meaning that there are six values for $v_{1_{\text{crit}}}$. It turns out that two of these critical angle parameters are those for which the collineation axis is perpendicular to the centreline of the coupler while four are two pairs of complex conjugates, which do not place P_{13} at infinity, given the way Equation (31) is derived.

To identify the joint angle parameters that locate P_{13} where the coupler centreline, the collineation axis, and the x_0-axis all intersect in a point at infinity we must adopt a different strategy: in this case P_{13} has a non-zero y_0-coordinate. Both configurations where the collineation axis, coupler, and x_0-axis are all parallel impose two useful conditions on the joint angle parameters.

The first condition requires that

$$\theta_1 + \theta_2 \quad = \quad 2\pi. \quad (33)$$

Converting this condition to its algebraic form leads to the very convenient result

$$\textbf{Condition 1}: \quad v_1 + v_2 \quad = \quad 0. \quad (34)$$

We can use Equation (6), the v_1-v_2 IO equation, to identify two values of $v_{1_{\text{crit}}}$. To do this, we solve Equation (6) for v_2:

$$v_2 = \frac{-4a_2a_4v_1 \pm \sqrt{((A_1B_1v_1^2+C_2D_2)(A_2B_1v_1^2+A_1C_1))}}{A_1B_1v_1^2+C_1D_2}. \quad (35)$$

Substitute each result into Equation (34) in order to obtain two quadratic equations in v_1, one pair for each assembly mode.

As previously mentioned, for the drag-link mechanism there is one configuration where the coupler, collineation axis, and the x_0-axis are all parallel that requires links a_1 and a_3 to cross each other. Figure 7 illustrates a drag-link mechanism in both the upper convex and lower complex quadrangle configurations. In order for Condition 1 to be true in both configurations, we must measure θ_2 with respect to the negative a_2 direction when links a_1 and a_3 cross.

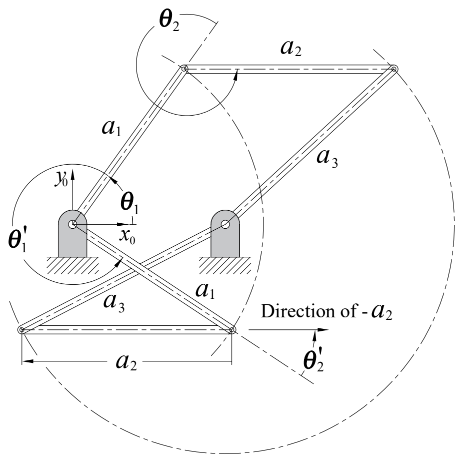

Fig. 7. The collieation axis and coupler are parallel to the x_0-axis.

The second condition requires the coupler-connected ends of links a_1 and a_3 to have the same y_0-coordinate values. This means that

$$a_1 \sin\theta_1 - a_3 \sin\theta_4 \quad = \quad 0 \tag{36}$$

which becomes

$$\textbf{Condition 2}: \quad a_1\frac{2v_1}{1+v_1^2} - a_3\frac{2v_4}{1+v_4^2} \quad = \quad 0 \tag{37}$$

using the tangent half-angle equivalents. Solving Equation (37) for v_4 yields

$$v_4 = \frac{a_3(1+v_1^2) \pm \sqrt{a_3^2(v_1^4+2v_1^2+1) - 4a_1v_1^2}}{2a_1v_1}. \tag{38}$$

Having first obtained v_1 from Equations (34) and (35), it is remarkably straightforward to determine the corresponding v_4 with Equation (38).

These two conditions, unique to the two configurations where the collineation and x_0-axes along with the coupler are all parallel, can be used to identify the required values for θ_1 and θ_4, and are summarised in Table II.

TABLE II

CONDITIONS FOR COUPLER BEING PARALLEL TO x_0-AXIS.

Condition 1	$v_1 + v_2 = 0$
Condition 2	$v_4 = \frac{a_3(1+v_1^2) \pm \sqrt{a_3^2(v_1^4+2v_1^2+1) - 4a_1v_1^2}}{2a_1v_1}$

We will now consider an example of locating the extreme values of P_{13} for a drag-link where P_{13} has four extreme values, two finite and two at infinity. However, the two at infinity do not, in general, represent extreme velocity ratios, rather they represent configurations where the input and output links instantaneously possess the same angular velocity magnitudes.

Using the link lengths already listed in Table I and applying the critical values for v_1 in Equation (32) we obtain the extreme finite values for P_{13}. Then to identify the critical values for v_1 that place P_{13} at infinity where the coupler as well as the collineation and x_0-axes intersect, we use Equations (34) and (35). It is a simple matter to compute the corresponding joint angles. The results are listed in Table III. These are the same results as illustrated in Figures 4-6.

VI. ACCELERATION LEVEL KINEMATICS

The acceleration level IO equations express the angular acceleration parameter generated by joint angle parameter v_i in terms of v_j. The $\ddot{v}_1$-$\ddot{v}_4$ IO equation expresses $\ddot{v}_4$ in terms of $\ddot{v}_1$ at any instant in time as a function of the configuration at that time. That is, if a set of numerical values for four constant link lengths a_1-a_4 are given in a feasible state of numerical values for v_1, v_4, $\dot{v}_1$, $\dot{v}_4$, and $\ddot{v}_1$, then $\ddot{v}_4$ is determined. This in turn means that if the mass centres and distributions are known, the extreme values for $\ddot{v}_1$, and $\ddot{v}_4$ can be used to identify the extreme values of the bearing reaction forces generated by the motion.

According to Freudenstein in [7], the maximum output angular acceleration, assuming constant input angular velocity is computed first for a crank-rocker then drag-link as

$$\ddot{\theta}_{4_{\max}} = \frac{\dot{\theta}_1^2 a_1}{a_2 a_3}(a_1+a_2) \quad \text{and} \quad \frac{\dot{\theta}_1^2 a_4}{a_2 a_3}(a_2+a_4). \tag{39}$$

But the configuration conditions he lists in the paper are incorrect, and the crank-rocker and drag-link he uses in an example are actually both non-Grashof double-rockers. We have developed a novel method using Equation (40), but it will require its own publication. Instead, we present an illustration with an example.

The time derivative of Equation (11) is

$$\begin{aligned} &((Av_4^2+B)v_1 - 4a_1a_3v_4)\ddot{v}_1 + \\ &\qquad ((Av_1^2+C)v_4 - 4a_1a_3v_1)\ddot{v}_4 + \\ &(Av_4^2+B)\dot{v}_1^2 + (Av_1^2+C)\dot{v}_4^2 + (4Av_1v_4 - 8a_1a_3)\dot{v}_1\dot{v}_4. \end{aligned} \tag{40}$$

The angular acceleration parameters, $\ddot{v}_i$, are related to the

TABLE III

RESULTS FOR EXTREMA EXAMPLE.

$\theta_{1_{\mathrm{crit}_1}}$	-154.3136°	P_{13_1}	-4.6987	$\left(\dot{\theta}_4/\dot{\theta}_1\right)_1$	0.7014
$\theta_{1_{\mathrm{crit}_2}}$	-11.7026°	P_{13_2}	4.6987	$\left(\dot{\theta}_4/\dot{\theta}_1\right)_2$	1.7411
$\theta_{1_{\mathrm{crit}_3}}$	54.9004°	P_{13_3}	∞	$\left(\dot{\theta}_4/\dot{\theta}_1\right)_3$	1
$\theta_{1_{\mathrm{crit}_4}}$	-71.7900°	P_{13_4}	∞	$\left(\dot{\theta}_4/\dot{\theta}_1\right)_4$	1

angular accelerations, $\ddot{\theta}_i$, as

$$\ddot{\theta}_i = \frac{2\ddot{v}_i}{(1+v_i^2)} - \dot{\theta}_i^2 v_i. \quad (41)$$

The five other angular acceleration parameter equations are

$$\begin{aligned}&((A_1B_1v_2^2 + A_2B_2)v_1 + 4a_2a_4v_2)\ddot{v}_1 + \\ &((A_1B_1v_1^2 + C_1D_2)v_2 + 4a_2a_4v_1)\ddot{v}_2 + \\ &(A_1B_1v_2^2 + A_2B_2)\dot{v}_1^2 + (A_1B_1v_1^2 + C_1D_2)\dot{v}_2^2 + \\ &(4A_1B_1v_1v_2 + 8a_2a_4)\dot{v}_1\dot{v}_2, \end{aligned} \quad (42)$$

$$\begin{aligned}&(A_2B_1v_3^2 + A_1B_2)v_1\ddot{v}_1 + (A_2B_1v_1^2 + C_1D_1)v_3\ddot{v}_3 + \\ &(A_2B_1v_3^2 + A_1B_2)\dot{v}_1^2 + (A_2B_1v_1^2 + C_1D_1)\dot{v}_3^2 + 4A_2B_1v_1v_3\dot{v}_1\dot{v}_3, \end{aligned} \quad (43)$$

$$\begin{aligned}&((B_1C_1v_3^2 + A_1D_2)v_2 - 4a_1a_3v_3)\ddot{v}_2 + \\ &((B_1C_1v_2^2 + A_2D_1)v_3 - 4a_1a_3v_2)\ddot{v}_3 + \\ &(B_1C_1v_3^2 + A_2D_1)\dot{v}_2^2 + (B_1C_1v_2^2 + A_2D_1)\dot{v}_3^2 + \\ &(4B_1C_1v_2v_3 - 8a_1a_3)\dot{v}_2\dot{v}_3, \end{aligned} \quad (44)$$

$$\begin{aligned}&(A_1C_1v_4^2 + B_1D_2)v_2\ddot{v}_2 + (A_1C_1v_2^2 + A_2C_2)v_4\ddot{v}_4 + \\ &(A_1C_1v_4^2 + B_1D_2)\dot{v}_2^2 + (A_1C_1v_2^2 + A_2C_2)\dot{v}_4^2 + 4A_1C_1v_2v_4\dot{v}_2\dot{v}_4, \end{aligned} \quad (45)$$

$$\begin{aligned}&((A_2C_1v_4^2 + B_1D_1)v_3 + 4a_2a_4v_4)\ddot{v}_3 + \\ &((A_2C_1v_3^2 + A_1C_2)v_4 + 4a_2a_4v_3)\ddot{v}_4 + \\ &(A_2C_1v_4^2 + B_1D_1)\dot{v}_3^2 + (A_2C_1v_3^2 + A_1C_2)\dot{v}_4^2 + \\ &(4A_2C_1v_3v_4 + 8a_2a_4)\dot{v}_3\dot{v}_4. \end{aligned} \quad (46)$$

We now continue the example whose results are listed in Table III and identify the maximum value for the output angular acceleration, $\ddot{\theta}_4$. Without loss of generality we assign a constant angular velocity for the input link of $\dot{\theta}_1 = 10$ rad/s. The results are listed in Table IV and illustrated in Figure 8.

TABLE IV
MAXIMUM $\ddot{\theta}_4$ RESULTS.

$\theta_{1_{\mathrm{crit}_1}}$	=	12.3685°	$\theta_{1_{\mathrm{crit}_2}}$	=	-39.4289°
$\dot{\theta}_{4_{\mathrm{crit}_1}}$	=	14.7804 rad/s	$\dot{\theta}_{4_{\mathrm{crit}_2}}$	=	14.3701 rad/s
$\ddot{\theta}_{4_{\mathrm{max}_1}}$	=	96.1559 rad/s^2	$\ddot{\theta}_{4_{\mathrm{max}_2}}$	=	-92.5833 rad/s^2

VII. CONCLUSIONS

The main contributions of this paper are the velocity and acceleration level kinematics results for any planar 4R linkage considering the six distinct relative angle parameter pairings, v_i-v_j. The algebraic velocity ratio equations result in a signed number, thereby indicating the relative sense of the two angular velocities. Using Freudenstein's generalised velocity ratio theorem and the four distinct Aronhold-Kennedy lines of ICVs reveals but four values of the six possible ratios. These results are very easy to use in any computer algebra system, such as Maple, for function generation and velocity ratio synthesis and analysis.

The ease and efficiency with which one may determine angular velocity and acceleration extreme values of such linkages suggests this formulation is very well suited for teaching senior mechanical engineering undergraduates in their upper year *Dynamics of Mechanisms* courses. Since we directly determine the extreme angular velocities and accelerations, determining inertial reaction forces in the frame-attached bearings is made significantly easier.

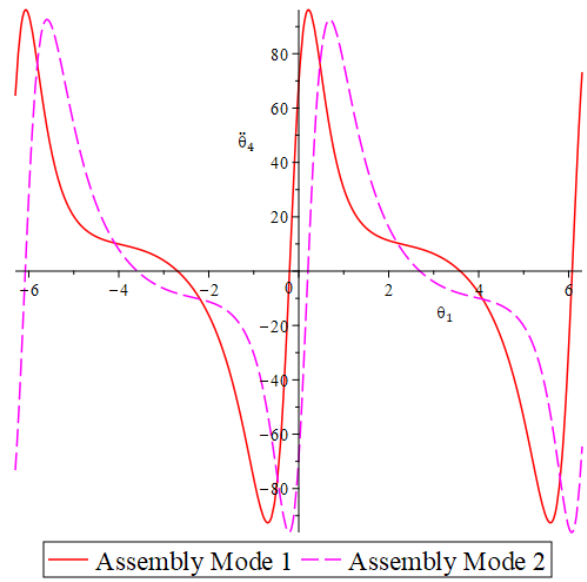

Fig. 8. Output angular acceleration $\ddot{\theta}_4$ versus input angle θ_1.

REFERENCES

[1] F. Freudenstein, "An Analytical Approach to the Design of Four-link Mechanisms." *Trans. ASME*, vol. 77, pp. 483–492, 1954.
[2] R. L. Norton, *Design of Machinery, Fifth Edition*. McGraw-Hill, New York, NY, USA, 2012.
[3] S. Bai and J. Angeles, "A Unified Input–output Analysis of Four-bar Linkages," *Mechanism and Machine Theory*, vol. 43(2), pp. 240–251, 2008.
[4] Q. Ge, Purwar, A., Zhao, P., and S. Deshpande, "A Task-Driven Approach to Unified Synthesis of Planar Four-Bar Linkages Using Algebraic Fitting of a Pencil of G-Manifolds," *Journal of Computing and Information Science in Engineering*, vol. 17(3), 2019.
[5] M. Rotzoll, M. J. D. Hayes, M. L. Husty, and M. Pfurner, "A General Method for Determining Algebraic Input-output Equations for Planar and Spherical 4R Linkages." Advances in Robotic Kinematics 2020, eds. Lenarčič, J. and Parenti-Castelli, V., Springer Nature Switzerland AG, Cham, Switzerlnd, 2020, pp. 96–97.
[6] M. Rotzoll, Q. Bucciol, and M. J. D. Hayes, "Algebraic Input-output Angle Equation Derivation Algorithm for the Six Distinct Angle Pairings in Arbitrary Planar 4R Linkages." *Submitted to* 20th International Conference on Advanced Robotics, Ljubljana, Slovenia, December 6-10, 2021.
[7] F. Freudenstein, "On the Maximum and Minimum Velocities and the Accelerations in Four-link Mechanisms," *Trans. ASME*, vol. 78, pp. 779–787, 1956.
[8] L. I. Wu and S. H. Wu, "A Note on Freudenstein's Theorem," *Mechanism and Machine Theory*, vol. vol 33, no. 1/2, pp. 139–149, 1998.
[9] F. Reuleaux, *The Kinematics of Machinery: Outlines of a Theory of Machines,* translated and edited by A.B.W. Kennedy. MacMillan and Co., London, England, 1876.
[10] A. S. Hall, *Kinematics and Linkage Design*. Prentice-Hall, Inc., Englewood Cliffs, N.J., U.S.A., 1961.
[11] R. Hartenberg and J. Denavit, *Kinematic Synthesis of Linkages*. McGraw-Hill, Book Co., New York, N.Y., U.S.A., 1964.
[12] J. M. McCarthy and G. S. Soh, *Geometric Design of Linkages, 2nd Edition* Interdiciplinary Applied Mathematics. Springer, New York, N.Y., 2011.